

Spectral Filtering for Learning Quantum Dynamics

Elad Hazan^{1,2} Annie Marsden²

Abstract

Learning high-dimensional quantum systems is a fundamental challenge that notoriously suffers from the curse of dimensionality. We formulate the task of predicting quantum evolution in the linear response regime as a specific instance of learning a Complex-Valued Linear Dynamical System (CLDS) with sector-bounded eigenvalues—a setting that also encompasses modern Structured State Space Models (SSMs).

While traditional system identification attempts to reconstruct full system matrices (incurring exponential cost in the Hilbert dimension), we propose Quantum Spectral Filtering, a method that shifts the goal to improper dynamic learning. Leveraging the optimal concentration properties of the Slepian basis, we prove that the learnability of such systems is governed strictly by an effective quantum dimension k^* , determined by the spectral bandwidth and memory horizon. This result establishes that complex-valued LDSs can be learned with sample and computational complexity independent of the ambient state dimension, provided their spectrum is bounded.

1. Introduction

Learning the dynamics of a quantum system—specifically its Hamiltonian or Liouvillian—from experimental observations is a cornerstone challenge in quantum science, which notoriously suffers from the curse of dimensionality. A system with n qubits implies a Hilbert space of dimension 2^n , and a Liouville space of dimension 4^n .

Instead of system identification, we focus on the prediction task of the next measurement from past observations. This falls into the framework of *dynamic learning* (Hazan et al., 2025), motivated by large language models, where the goal is purely performative in terms of next token prediction.

¹Department of Computer Science, Princeton University

²Google DeepMind Princeton. Correspondence to: Elad Hazan <elad.hazan@gmail.com>.

Connection to Learning Complex-Valued Dynamical Systems.

Beyond quantum physics, the formulation studied in this paper naturally arises in modern machine learning as the problem of learning *complex-valued linear dynamical systems* (CLDSs). Such systems are increasingly used to model oscillatory and long-range temporal dependencies in sequence data, appearing in linear recurrent neural networks, structured state space models (SSMs), and spectral sequence models. In these settings, complex-valued eigenvalues enable efficient representation of phase information and periodic structure, but also pose fundamental challenges for learnability due to slow spectral decay and long memory.

1.1. Problem Setup

Our primary objective is to sequentially predict a sequence of observations y_1, \dots, y_t, \dots according to the mean square error, $\sum_t \|y_t - \hat{y}_t\|^2$. The observations were generated by a quantum dynamical system in the **linear response formulation**. While generic quantum evolution can be bilinear in state and controls, we focus on the standard learning regime of *linear response*, where controls u_t are small perturbations from a steady state. In this regime, by vectorizing the density matrix, the dynamics map exactly to a classical Linear Time-Invariant (LTI) system:

$$y_t = \sum_{\tau=1}^{\infty} CA^{\tau-1} Bu_{t-\tau}, \quad (1)$$

where A is the Liouvillian superoperator governing free evolution, B is the control superoperator, and C is the vectorized observable (representing the trace operation of a measurement as a linear functional), see exposition in e.g. (Breuer & Petruccione, 2002). Very importantly, these objects lie in **very high dimension**, and it is desirable to design algorithms that depend mildly, say logarithmically, on the dimension. In this work we consider a finite impulse response with memory up to W ,

$$y_t = \sum_{\tau=1}^W CA^{\tau-1} Bu_{t-\tau}.$$

We further assume spectral assumptions on A . Specifically, we require that the spectrum of A is contained within the *spectral sector* \mathbb{C}_β :

$$\mathbb{C}_\beta \triangleq \{z \in \mathbb{C} \mid |z| \leq 1, |\arg(z)| \leq \beta\}. \quad (2)$$

This condition ensures the system is stable (eigenvalues within the unit disk) and limits the maximum oscillation frequency to β . In appendix C we describe how this formulation relates to the Schrödinger equation and other quantum formulations.

1.2. Main Results

We give an efficient algorithm, detailed in Algorithm 1, based on a novel variant of spectral filtering, whose performance is bounded as follows (the precise statement appears in Corollary 5.2): Let $\{y_t\}_{t=1}^T$ be a sequence of observations generated by a noiseless quantum system whose transition operator has all eigenvalues in \mathbb{C}_β and whose memory of the previous observations is bounded by W observations. Then Algorithm 1 produces a sequence of causal predictions $\{\hat{y}_t\}$ such that:

$$\frac{1}{T} \sum_{t=1}^T |\hat{y}_t - y_t|^2 \leq \tilde{O} \left(\frac{\beta W \log^2 T}{T} \right).$$

Importantly, our algorithm has the following properties:

1. Most importantly, its running time and performance guarantee do not depend on the hidden dimension of the dynamical system. Our analysis reveals that this dimensionality reduction is not a quantum accident, but a manifestation of the classical ‘‘Shannon number’’ phenomenon found in time-frequency analysis, governed by the spectral concentration of Discrete Prolate Spheroidal Sequences (DPSS) (Slepian, 1978).
2. The number of learned parameters does not depend on the memory window parameter W . The running time of the algorithm can be made to depend logarithmically on W , as per (Agarwal et al., 2024).

We note that for a system with memory bound of W observations, one could apply simple regression to dynamically learn and predict. Applying online linear regression (see e.g. (Cesa-Bianchi & Lugosi, 2006; Hazan, 2022)) would give a regret of

$$\frac{1}{T} \sum_{t=1}^T |\hat{y}_t - y_t|^2 \leq \tilde{O} \left(\frac{W \log T}{T} \right).$$

However, this would require W parameters, memory, and run time which is quadratic in W .

We also show in Appendix A that when β is assumed to be a constant, a regret of $\Omega(\frac{W}{T})$ is inevitable for any algorithm, regardless of computational efficiency, via an information-theoretic argument.

2. Related Work

System Identification and Tomography. The characterization of quantum dynamics is traditionally framed as a parameter estimation problem. Standard Quantum Process Tomography (QPT) reconstructs the full superoperator, scaling as $O(d^4)$ for a d -dimensional Hilbert space (Nielsen & Chuang, 2010). To mitigate this, Compressed Sensing (Gross et al., 2010) and Matrix Completion (Flammia et al., 2012) exploit low-rank assumptions to reduce sample complexity. In the specific context of linear dynamical systems, (Guță & Yamamoto, 2016) and (Levitt & Guță, 2017) developed identification theories for passive linear quantum systems. However, these approaches still aim to explicitly recover system parameters (the A, B, C matrices), which is often computationally prohibitive and unnecessary for prediction tasks.

Control-Theoretic Approaches. Linear Dynamical Systems (LDS) appear extensively in quantum control theory, providing the physical justification for the LTI formulation used in this work. (Nurdin et al., 2009) established the theory for the network synthesis of linear quantum stochastic systems, deriving conditions under which an LTI system corresponds to a physically realizable quantum device. This formalism underpins Quantum Kalman Filtering (Wiseman & Milburn, 2009), where the goal is real-time state estimation rather than parameter learning.

Learning-Theoretic Perspectives. From a learning perspective, (Aaronson et al., 2018) introduced the framework of online learning for quantum states, providing regret bounds for predicting measurements on a sequence of states. Our work extends this philosophy from estimating states to learning the full dynamical evolution. A related advancement is Shadow Tomography (Aaronson, 2018; Huang et al., 2020), which predicts properties of a quantum state using few measurements. While Shadow Tomography addresses static properties via i.i.d. resets, it does not address the problem of predicting the future evolution of a single, non-stationary dynamical system from a continuous trajectory, which is the focus of our spectral filtering approach.

Improper Learning. Our work departs from the identification paradigm by focusing on *improper learning*—predicting future observations without explicit reconstruction of the Liouvillian. While recent algorithms have addressed quantum linear system solving (Li et al., 2022), they generally assume access to the system matrices. In contrast, our spectral filtering approach operates in the agnostic setting, leveraging the spectral decay of the Liouvillian to circumvent the curse of dimensionality.

Neural architectures and Complex LDS. It is known that it is a difficult problem to learn a complex LDS, i.e. a linear dynamical system whose hidden transition matrix may be asymmetric and have complex eigenvalues. While many methods do exist (see (Ghai et al., 2020) and (Bakshi et al., 2023) for example), their regret guarantees grow linearly with the hidden dimension, which can be prohibitively large.

(François et al., 2025) consider the problem of learning a linear dynamical system in the presence of complex eigenvalues in a restricted setting— they consider only systems that correspond to the shift operation (in other words, they consider systems whose hidden transition matrix is a shift-permutation matrix). They prove tight bounds that relate the accuracy of retrieval to the ratio of the state dimension to the retrieval horizon. This corresponds to the ‘Information Cutoff’ we derive in our main theorem, where the effective quantum dimension k^* is determined by the product of the spectral bandwidth β and the observation window W . While (François et al., 2025) construct specific parameterizations to approximate the retrieval operator, our approach is significantly more general. We provide a universal learning algorithm that captures any dynamical evolution within the spectral sector \mathbb{C}_β .

(Marsden & Hazan, 2025) introduces the method of *universal sequence preconditioning* and shows that combining this technique with linear regression allows for sublinear regret in the presence of a complex LDS that is dimension-free up to logarithmic factors. However, the convergence guarantees are restricted to the regime where the spectral bandwidth β is bounded by $1/\text{poly}(\log T)$. In contrast, our Quantum Spectral Filtering approach utilizes the Slepian basis, which is optimally concentrated for any β . This allows us to characterize the learnability of the system directly through the effective quantum dimension $k^* \approx \beta W/\pi$, providing a more general treatment of the spectral sector without requiring the bandwidth to vanish with the time horizon. That said, we do require a finite window W whereas Marsden & Hazan (2025) consider the regime where $W = T$.

Our development of complex-valued spectral filtering is further motivated by recent theoretical results on Structured State Space Models (SSMs). (Ran-Milo et al., 2024) established a fundamental separation between real and complex parameterizations, proving that real-valued diagonal SSMs cannot efficiently approximate oscillatory dynamics—a core feature of quantum evolution—without incurring an exponential cost in parameter magnitude or dimension. Complementing this, (Orvieto et al., 2023) identify a conditioning bottleneck in real-valued recurrences, proving that complex eigenvalues are strictly necessary to ensure the memory retrieval map remains well-conditioned over long horizons.

3. Theoretical Framework

The Quantum Information Matrix. Let the dynamics of a generic mode of a quantum system be governed by a complex eigenvalue $z \in \mathbb{C}_\beta$. We define the *Quantum Information Matrix* $Z_W(\beta) \in \mathbb{C}^{W \times W}$ as the Gram matrix of all realizable monomial trajectories $\mu_W(z) = [1, z, z^2, \dots, z^{W-1}]^\top$ of length W over this sector, under a uniform prior:

$$Z_W(\beta) \triangleq \int_{\mathbb{C}_\beta} \mu_W(z) \mu_W(z)^\dagger dA(z), \quad (3)$$

where $dA(z) = r dr d\theta$ is the area measure. This matrix encapsulates the total correlations available to any learning algorithm observing the system for a window of W steps. Evaluating this integral yields:

$$(Z_W(\beta))_{jk} = \frac{2\beta}{j+k+2} \cdot \text{sinc}((j-k)\beta). \quad (4)$$

The mathematical structure of $Z_W(\beta)$ naturally separates the non-unitary (dissipative) parts of the dynamics from the unitary (Hamiltonian) parts as $Z_W(\beta) = A \circ B$ where

- Dissipative Component (A):** A Hankel matrix with entries $A_{jk} = \frac{1}{j+k+2}$. This component depends only on $j+k$, representing radial decay characteristic of open systems.
- Unitary Component (B):** A Toeplitz matrix with entries $B_{jk} = 2\beta \cdot \text{sinc}((j-k)\beta)$. This component depends only on $j-k$, representing time-translation invariant (unitary) evolution.

This can be seen by evaluating the entry $(Z_W(\beta))_{jk}$ using polar coordinates $z = re^{i\theta}$, separating the radial (dissipative) and angular (unitary) integrals:

$$(Z_W(\beta))_{jk} = \left(\int_0^1 r^{j+k+1} dr \right) \cdot \left(\int_{-\beta}^{\beta} e^{i(j-k)\theta} d\theta \right).$$

The first term is purely radial, yielding the Hankel matrix $A_{jk} = \frac{1}{j+k+2}$. The second term is purely angular, yielding the Toeplitz matrix $B_{jk} = \int_{-\beta}^{\beta} e^{i(j-k)\theta} d\theta = 2\beta \cdot \text{sinc}((j-k)\beta)$, which is recognized as the prolate spheroidal (Slepian) kernel governing band-limited signals (Slepian, 1978).

3.1. Quantum Eigen-Phase Transition

A central consequence of the spectral structure of the Quantum Information Matrix $Z_W(\beta)$ is the emergence of a sharp phase transition in its singular value spectrum. This transition determines the number of degrees of freedom of a quantum dynamical system that can be reliably learned from a finite observation window.

This phenomenon is closely related to the classical theory of time–frequency concentration: a signal that is band-limited in frequency and observed over a finite horizon possesses only a finite number of effective degrees of freedom. In signal processing, this quantity is known as the *Shannon number*, and it governs the rank of the optimal time–frequency concentration operator. In our setting, the same principle manifests itself in the spectrum of $Z_W(\beta)$.

Definition 3.1 (Effective Quantum Dimension). The effective quantum dimension of an observation window of length W with spectral bound β is defined as

$$k^* \triangleq \left\lceil \frac{\beta}{\pi} W \right\rceil.$$

The quantity k^* admits a natural interpretation: it is the maximal number of independent oscillatory modes whose phases can be resolved over W time steps when the spectrum of the dynamics is confined to the sector C_β . Equivalently, k^* coincides with the Shannon number of a band-limited discrete-time signal with bandwidth β observed over a window of length W .

The following theorem formalizes this intuition by showing that $Z_W(\beta)$ exhibits a sharp *information cutoff* at the effective dimension k^* .

Theorem 3.2 (Information Cutoff). *Let $Z_W(\beta) \in \mathbb{C}^{W \times W}$ be the Quantum Information Matrix, and let*

$$k^* := \left\lceil \frac{\beta}{\pi} W \right\rceil.$$

There exist constants $C, c > 0$ such that for all $k \geq k^$,*

$$\sigma_k(Z_W(\beta)) \leq C \exp\left(-c k/k^*\right).$$

This result implies that, although the ambient state dimension of the quantum system may be exponentially large, the information accessible from observations over a finite horizon is effectively confined to a k^* -dimensional subspace. Beyond this threshold, additional spectral components contribute only exponentially small information and are therefore fundamentally unlearnable from data. \square

Proof Sketch. The matrix $Z_W(\beta)$ decomposes as a Hadamard product $Z_W(\beta) = A \circ B$, where A is a Hankel matrix with exponentially decaying spectrum and B is a Toeplitz (DPSS) matrix with effective rank k^* . A generalized eigenvalue tail bound for Hadamard products implies that truncating A at rank s and B at rank k^* yields rank at most sk^* . Combining this with the exponential decay of A and the sharp spectral concentration of B gives $\sigma_{sk^*+1}(Z_W(\beta)) \lesssim e^{-cs}$, which implies the stated stretched-exponential decay. The full proof appears in Appendix B. \square

Figure 1 empirically illustrates this sharp transition for a window of $W = 200$ observations at two different energy band limits.

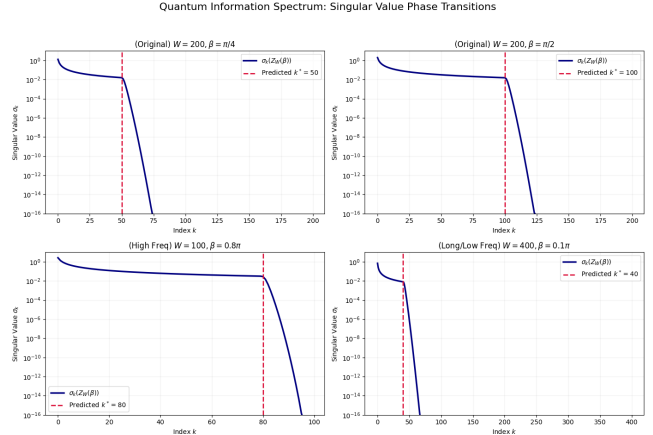


Figure 1. Quantum Information Spectrum. Singular values of $Z_W(\beta)$ for $W = 100, 200, 400$ on a log scale. The red vertical lines indicate the theoretical Quantum Sampling limit $k^* = \lceil \frac{\beta}{\pi} W \rceil$, marking the boundary between learnable signal and noise.

4. Algorithm: Quantum Spectral Filtering

Our theoretical analysis implies that any trajectory of length W generated by a quantum system within the spectral sector C_β can be efficiently represented in the low-dimensional subspace spanned by the principal eigenvectors of $Z_W(\beta)$. We leverage this to formulate the *Quantum Spectral Filtering* algorithm.

4.1. Optimal Basis Construction

Let $Z_W(\beta) = \sum_{i=1}^W \sigma_i v_i v_i^\dagger$ be the eigendecomposition of the Quantum Information Matrix, with singular values sorted $\sigma_1 \geq \sigma_2 \geq \dots \geq \sigma_W$. According to Theorem 3.2 (Information Cutoff), the subspace $\mathcal{V}_{k^*} = \text{span}\{v_1, \dots, v_{k^*}\}$ captures the system’s dynamics with exponentially small error. We define our spectral filter bank $\Phi \in \mathbb{C}^{W \times k^*}$ using these top k^* eigenvectors:

$$\Phi \triangleq [v_1, v_2, \dots, v_{k^*}]. \quad (5)$$

These filters v_i are fixed *a priori* based solely on the observation window W and the assumed energy/decoherence scale β .

4.2. Learning via Filtering

We treat the sequence of controls and observations as a time series. At any time t , the history window of controls $U_t \in \mathbb{C}^W$ is projected onto the optimal subspace. We employ a generic online learning algorithm \mathcal{A} (such as Online

Ridge Regression or VAW) to learn the dynamics in this compressed space.

Algorithm 1 Quantum Spectral Filtering (Generic Online)

```

1: Input: Window  $W$ , Horizon  $T$ , Spectral bound  $\beta$ , Base
   online algorithm  $\mathcal{A}$ 
2: Initialize:
3:   Compute effective dimension  $k^* = \lceil \frac{\beta}{\pi} W \rceil$ 
4:   Compute top  $k^*$  eigenvectors of  $Z_W(\beta)$  to form filter
   bank  $\Phi \in \mathbb{C}^{W \times k^*}$ 
5:   Initialize base algorithm  $\mathcal{A}$  in dimension  $k^*$ 
6: for  $t = 1, 2, \dots, T$  do
7:   Observe control history  $U_t = [u_t, u_{t-1}, \dots, u_{t-W+1}]^\top \in \mathbb{C}^W$  (zero-padded
   if  $t < W$ )
8:   Filter: Compute compressed state  $h_t = \Phi^\dagger U_t \in \mathbb{C}^{k^*}$ 
9:   Predict: Query  $\mathcal{A}$  with input  $h_t$  to get prediction
    $\hat{y}_{t+1}$ 
10:  Observe true next value  $y_{t+1}$ 
11:  Update: Update  $\mathcal{A}$  with observation pair  $(h_t, y_{t+1})$ 
12: end for

```

5. Performance Guarantees

Henceforth we assume the *realizable* setting, where the observations are generated by a generic quantum system with dynamics constrained to the spectral sector \mathbb{C}_β .

Theorem 5.1 (Generative Learning Guarantee). *Let $\{y_t\}_{t=1}^T$ be a sequence of observations generated by a noiseless quantum system whose transition operator has all eigenvalues in \mathbb{C}_β and whose memory is bounded by W . If Algorithm 1 is run with a filter bank of size k using the Vovk-Azoury-Warmuth (VAW) update rule defined by:*

$$\hat{y}_t = h_t^* \left(\lambda I_k + \sum_{s=1}^t h_s h_s^* \right)^{-1} \sum_{s=1}^{t-1} y_s h_s, \quad (6)$$

then its total cumulative squared prediction error satisfies:

$$\sum_{t=1}^T |\hat{y}_t - y_t|^2 \leq \tilde{O}(k \log T) + \tilde{O}(T \cdot (\beta W)^3 \cdot \exp(-ck/k^*)), \quad (7)$$

where $k^* = \lceil \frac{\beta}{\pi} W \rceil$ is the effective quantum dimension and $C' > 0$ is a universal constant.

A significant and immediate corollary from this theorem is as follows:

Corollary 5.2 (Fast Convergence Rates). *Let $\{y_t\}_{t=1}^T$ be a sequence of observations generated by a noiseless quantum system whose transition operator has all eigenvalues in \mathbb{C}_β and whose memory is bounded by W . Then Algorithm 1*

with filter bank size $k = \Theta(\frac{\beta}{\pi} W \log(T\beta W))$ attains an average regret of:

$$\frac{1}{T} \sum_{t=1}^T |\hat{y}_t - y_t|^2 \leq \tilde{O}\left(\frac{\beta W \log^2(T\beta W)}{T}\right).$$

6. Analysis of Main Theorem

The proof of our theorem makes use of the following theorem from (Marsden & Hazan, 2025).

Theorem 6.1 (Proof of Lemma E.4¹ (Marsden & Hazan, 2025)). *Let $\{\phi_i\}_{i=1}^W$ be the eigenvectors of $Z_W(\beta)$ sorted by eigenvalue $\sigma_1 \geq \sigma_2 \geq \dots \geq \sigma_W$. For any $z \in \mathbb{C}_\beta$, the projection of its monomial trajectory onto the i -th basis vector decays with the corresponding eigenvalue σ_i as follows,*

$$\max_{z \in \mathbb{C}_\beta} |\phi_i^\dagger \mu_W(z)|^2 \leq (24 \cdot (12)^2 \beta^7 W^4 \sigma_i)^{1/3}. \quad (8)$$

Our analysis departs from that of (Marsden & Hazan, 2025) in that we prove and exploit much stronger spectral properties of the Quantum Information Matrix. Indeed, applying Theorem 3.2 to the above gives our final result.

Lemma 6.2 (Spectral Decay). *Let $\{\phi_i\}_{i=1}^W$ be the eigenvectors of $Z_W(\beta)$ sorted by eigenvalues $\sigma_1 \geq \sigma_2 \geq \dots \geq \sigma_W$. For any $z \in \mathbb{C}_\beta$, the projection of its monomial trajectory onto the i -th basis vector decays exponentially beyond the effective dimension: for $i > k^*$*

$$\max_{z \in \mathbb{C}_\beta} |\phi_i^\dagger \mu_W(z)|^2 \leq C \beta^{7/3} W^{4/3} \exp(-ci/k^*). \quad (9)$$

Detailed Proof of Theorem 5.1. We decompose the total cumulative error into *estimation error* (regret) and *approximation error* (bias). Let $w^* = \operatorname{argmin}_{w \in \mathbb{C}^k} \sum_{t=1}^T |w^\top h_t - y_t|^2$ be the best offline predictor in our chosen subspace Φ . The total error is:

$$\begin{aligned} \sum_{t=1}^T |\hat{y}_t - y_t|^2 &= \underbrace{\left(\sum_{t=1}^T |\hat{y}_t - y_t|^2 - \sum_{t=1}^T |w^*^\top h_t - y_t|^2 \right)}_{\text{Estimation Error}} \\ &\quad + \underbrace{\sum_{t=1}^T |w^*^\top h_t - y_t|^2}_{\text{Approximation Error}} \end{aligned}$$

1. Estimation Error (Special Case: VAW): We analyze the specific case where \mathcal{A} is the Vovk-Azoury-Warmuth (VAW) forecaster (also known as Forward-Step Ridge Regression). Following the analysis of Follow-The-Regularized-Leader (FTRL) with quadratic regularization

¹The result comes from combining Eq. 11 with Lemma A.1

(e.g., Orabona, 2019), the cumulative regret is bounded by the log-determinant of the data covariance matrix. For the square loss, the regret satisfies:

$$\mathcal{R}_T(w^*) \leq \lambda \|w^*\|^2 + \sum_{t=1}^T \log (1 + h_t^* V_{t-1}^{-1} h_t), \quad (10)$$

where $V_{t-1} = \lambda I_k + \sum_{s=1}^{t-1} h_s h_s^\dagger$ is the regularized covariance matrix. Using the Elliptical Potential Lemma, the sum term is exactly the log-ratio of determinants:

$$\sum_{t=1}^T \log(1 + h_t^* V_{t-1}^{-1} h_t) = \log \frac{\det(V_T)}{\det(\lambda I)}.$$

Assuming bounded inputs $\|h_t\|^2 \leq L^2$ within the subspace, the trace of the covariance matrix is bounded by $\text{Tr}(V_T) \leq k\lambda + TL^2$. By the AM-GM inequality, the determinant is maximized when the energy is distributed equally among the k eigenvalues:

$$\det(V_T) \leq \left(\frac{\text{Tr}(V_T)}{k} \right)^k \leq \left(\lambda + \frac{TL^2}{k} \right)^k.$$

Taking the logarithm yields the dimension-dependent bound:

$$\log \det(V_T) - k \log \lambda \leq k \log \left(1 + \frac{TL^2}{\lambda k} \right).$$

Thus, the estimation error scales linearly with the filter bank size k (not W):

$$\text{Estimation Error} \leq \tilde{O}(k \log T).$$

2. Approximation Error: We bound the error of the best linear predictor w^* in our basis. Assuming the system is a linear time-invariant (LTI) system driven by inputs u_t with memory W , the true observation is

$$y_{t+1} = \sum_{\tau=1}^W C A^{\tau-1} B u_{t-\tau+1} = \sum_{\tau=1}^W \bar{C} D^{\tau-1} \bar{B} u_{t-\tau+1},$$

where A is diagonalized into $A = PDP^{-1}$, for a diagonal matrix D , and P, P^{-1} are absorbed into $\bar{C} = CP, \bar{B} = P^{-1}B$. Let the d eigenvalues of A be $\{z_j\} \subset \mathbb{C}_\beta$, then we can write the true system as a linear combination of eigenvector products as:

$$y_{t+1} = \sum_{j=1}^d c_j \cdot \mu_W(z_j)^\top U_t,$$

where recall that $U_t = [u_t, u_{t-1}, \dots, u_{t-W+1}]$ (padded if necessary for $t < W$), $\mu_W(z) = [1, z, z^2, \dots, z^{W-1}]^\top$, and c_j is given by $c_j = \bar{C}_j^\top \bar{B}_j$.

We choose the ideal weights $w^* = \sum_{j=1}^d c_j (\Phi^\dagger \mu_W(z_j))$ to match the projection of these true parameters onto our basis Φ . The approximation error at time t is:

$$e_t = w^{*\top} h_t - y_{t+1} = - \sum_{j=1}^d c_j \sum_{i=k+1}^W (\phi_i^\dagger \mu_W(z_j)) (\phi_i^\top U_t)$$

Applying Cauchy-Schwarz and assuming bounded inputs, i.e. $\|u_t\|_2 \leq 1$ (so that $\|U_t\|^2 \leq W$):

$$\begin{aligned} |e_t|^2 &\leq \left(\sum_{j=1}^d |c_j| \sqrt{\sum_{i=k+1}^W |\phi_i^\dagger \mu_W(z_j)|^2} \sqrt{\sum_{i=k+1}^W |\phi_i^\top U_t|^2} \right)^2 \\ &\leq \left(\sum_{j=1}^d |c_j| \sqrt{\sum_{i=k+1}^W \max_{z \in \mathbb{C}_\beta} |\phi_i^\dagger \mu_W(z)|^2 \cdot \|U_t\|_2} \right)^2 \end{aligned}$$

Using Lemma 6.2, each term in the sum decays exponentially and the entire sum can be bounded by a multiple of its first term at $i = k + 1$.

$$\begin{aligned} |e_t|^2 &\leq \left(\|c\|_1 \cdot \sqrt{W \cdot (C\beta^{7/3}W^{4/3} \exp(-ck/k^*))} \right)^2 \\ &\leq C\|c\|_1^2 \beta^{7/3} W^{7/3} \exp(-ck/k^*). \end{aligned}$$

Notice that each term c_i can be bounded as $|c_i| = |\bar{C}_i| |\bar{B}_i| \leq |P| |P^{-1}| |C_i| |B_i|$. This is a constant which depends on the condition number of A , as well as the norms of the matrices B, C . Since eventually it will appear logarithmically in the choice of k , we consider it a constant. Moreover, since the powers of β and W will also appear only logarithmically we simplify them with an upper bound of $7/3 \leq 3$. Thus,

$$|e_t|^2 \leq CW^3\beta^3 \exp(-ck/k^*).$$

Summing this constant error bound over all T time steps yields the final approximation term. Combining these two terms yields the final generative bound. \square

7. Experimental Validation

7.1. Hamiltonian Tomography

Hamiltonian tomography is the inverse problem of inferring a quantum system's dynamical generator—its Hamiltonian and associated dissipative couplings—from observed time-evolution data. In the context of this paper, we do *improper* tomography, namely predict a sequence of observations y_t that were generated by (1), according to the mean square error.

To empirically validate the information-theoretic limit k^* derived in Theorem 1, we perform Hamiltonian tomography on a family of simulated quantum systems constrained to

the spectral sector \mathbb{C}_β . The goal is to demonstrate that the learnability of the dynamics is strictly governed by the effective quantum dimension $k^* = \lceil \frac{\beta}{\pi} W \rceil$, regardless of the ambient Hilbert space dimension.

We generate synthetic data from random Linear Time-Invariant (LTI) systems that adhere to the spectral constraints of our theory. For each trial, we construct a random dynamical system with hidden dimension $d = 20$ as follows:

- Spectral Constraint:** The eigenvalues of the transition matrix A are drawn uniformly from the sector $\mathbb{C}_\beta = \{z \in \mathbb{C} : 0.85 \leq |z| \leq 0.95, |\arg(z)| \leq \beta\}$.
- Finite Memory Generation:** We generate observations $\{y_t\}$ via a strictly bounded convolution of length $W = 100$. The ground truth observations are generated as $y_t = \sum_{\tau=1}^W CA^{\tau-1}Bu_{t-\tau}$, where the control inputs u_t are standard complex Gaussian noise.
- Data Splitting:** For each system, we generate a trajectory of length $T = 1000$, split into a training set ($T_{train} = 800$) and a held-out test set ($T_{test} = 200$).

We apply the Quantum Spectral Filtering algorithm (Algorithm 1) to learn the dynamics from the training data. For a fixed window size $W = 100$ and a given spectral band β , we pre-compute the universal filter bank $\Phi \in \mathbb{C}^{W \times W}$ consisting of the eigenvectors of the Information Matrix $Z_W(\beta)$.

We examine the model's performance as a function of the filter bank size K (the number of spectral features retained). For each $K \in \{5, 10, \dots, 95\}$, we project the input history onto the top K vectors of Φ and learn the linear map to the next observation using Ridge Regression ($\lambda = 10^{-5}$). We report the Test Mean Squared Error (MSE).

We evaluate the algorithm across three distinct spectral regimes: slow dynamics ($\beta = 0.2\pi$), intermediate dynamics ($\beta = 0.5\pi$), and fast dynamics ($\beta = 0.9\pi$). We report the mean MSE and 95% confidence intervals over 20 independent trials for each configuration.

The results, visualized in Figure 2, confirm a sharp phase transition in learnability. In all cases, the test error remains high (indicating a failure to learn) until the model capacity K approaches the theoretical effective dimension k^* . Once K exceeds k^* (indicated by the vertical dashed lines), the MSE plunges exponentially, hitting the numerical noise floor ($\sim 10^{-13}$). This confirms that the spectral filters spanning the subspace \mathcal{V}_{k^*} capture essentially 100% of the dynamical information.

For the low-bandwidth system ($\beta = 0.2\pi$, red curve), perfect learning is achieved with only $K = 20$ filters, despite

the window size being $W = 100$. This validates that the remaining 80 dimensions of the observation space contain no recoverable signal, allowing for significant data compression without loss of accuracy.

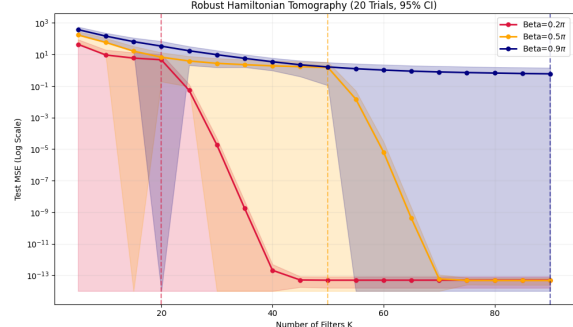


Figure 2. Robust Hamiltonian Tomography. Test MSE of the Quantum Spectral Filtering algorithm learning the dynamics of random quantum systems with window size $W = 100$. We vary the filter bank size K across three spectral bands: $\beta = 0.2\pi$ (red), $\beta = 0.5\pi$ (orange), and $\beta = 0.9\pi$ (navy). Solid lines represent the mean MSE over 20 independent trials, while shaded regions indicate the 95% confidence interval. Vertical dashed lines mark the theoretical effective dimension $k^* = \lceil \frac{\beta}{\pi} W \rceil$. The sharp phase transition at k^* confirms that the subspace \mathcal{V}_{k^*} captures the system's dynamics with high precision, while the negligible variance post-cutoff validates the universality of this limit.

7.2. Ablation Study: Effects of Hidden Dimension

A central claim of our theoretical framework is that the learnability of quantum dynamics is governed solely by the spectral properties of the system—specifically the effective quantum dimension k^* —rather than the ambient dimension of the Hilbert space. To empirically test this claim, we evaluated the performance of Quantum Spectral Filtering on systems with widely varying hidden state dimensions $d \in \{50, 200, 800\}$, while keeping the observation window ($W = 100$) and spectral bandwidth ($\beta = 0.5\pi$) constant. Note that a hidden dimension of $d = 800$ corresponds to a Liouvillian superoperator of size $d^2 = 640,000$. The results, illustrated in Figure 3, validate Theorem 3.2: the complexity of learning in the linear response regime is strictly determined by the spectral bandwidth and memory horizon, and not by the ambient dimension.

7.3. Ablation Study: Optimality of the Slepian Basis

A core theoretical contribution of this work is the identification of the Slepian (DPSS) basis as the optimal subspace for compressing quantum history. To rigorously justify the necessity of the Slepian basis, we performed an ablation study comparing our Quantum Spectral Filtering algorithm against a baseline variant that substitutes the filter bank Φ with the top- K low-frequency modes of the standard DFT matrix.

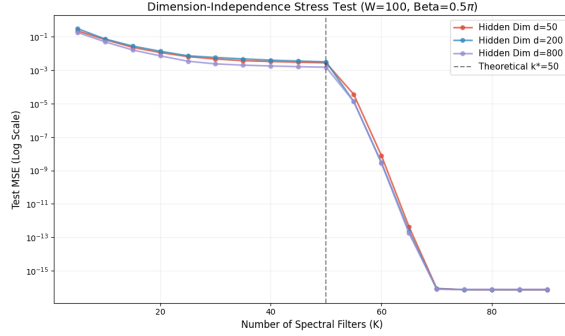


Figure 3. Effects of the Hidden Dimension.

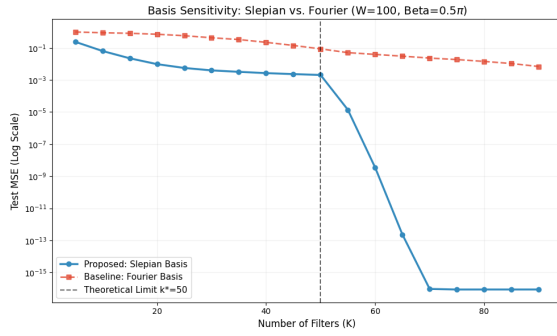


Figure 4. Basis Sensitivity: Slepian vs. Fourier.

We generated synthetic trajectories from a random complex-valued quantum system with hidden dimension $d = 100$, observation window $W = 100$, and spectral bandwidth $\beta = 0.5\pi$. Both the Slepian and Fourier variants were evaluated on their ability to predict future observations as a function of the subspace size K .

The results, presented in Figure 4, reveal a stark contrast in convergence efficiency. The proposed Slepian basis (blue curve) exhibits a sharp phase transition exactly at the theoretical information cutoff $k^* = 50$, driving the prediction error to the numerical precision floor. In contrast, the Fourier basis (red curve) converges significantly slower, suffering from a heavy tail of error due to the poor concentration of DFT modes on finite intervals.

Impact Statement

This paper presents work whose goal is to advance the field of Machine Learning. There are many potential societal consequences of our work, none which we feel must be specifically highlighted here.

References

Aaronson, S. Shadow tomography of quantum states. In *Proceedings of the 50th Annual ACM SIGACT Symposium on Theory of Computing*, pp. 325–338, 2018.

Aaronson, S., Chen, X., Hazan, E., Kale, S., and Nayak, A. Online learning of quantum states. In *Advances in Neural Information Processing Systems*, volume 31, 2018.

Agarwal, N., Chen, X., Dogariu, E., Shah, D., Strauss, H., Feinberg, V., Suo, D., Bartlett, P., and Hazan, E. Futurefill: Fast generation from convolutional sequence models. *arXiv preprint arXiv:2410.03766*, 2024.

Bakshi, A., Liu, A., Moitra, A., and Yau, M. A new approach to learning linear dynamical systems. In *Proceedings of the 55th Annual ACM Symposium on Theory of Computing*, pp. 335–348, 2023.

Beckermann, B. and Townsend, A. On the singular values of matrices with displacement structure. *SIAM Journal on Matrix Analysis and Applications*, 38(4):1227–1248, 2017.

Breuer, H.-P. and Petruccione, F. *The theory of open quantum systems*. OUP Oxford, 2002.

Cesa-Bianchi, N. and Lugosi, G. *Prediction, Learning, and Games*. Cambridge University Press, 2006. doi: 10.1017/CBO9780511546921.

Flammia, S. T., Gross, D., Liu, Y.-K., and Eisert, J. Quantum tomography via compressed sensing: error bounds, sample complexity and efficient estimators. *New Journal of Physics*, 14(9):095022, 2012.

François, A., Orvieto, A., and Bach, F. An uncertainty principle for linear recurrent neural networks. *arXiv preprint arXiv:2502.09287*, 2025.

Ghai, U., Lee, H., Singh, K., Zhang, C., and Zhang, Y. No-regret prediction in marginally stable systems. In *Conference on Learning Theory*, pp. 1714–1757. PMLR, 2020.

Gross, D., Liu, Y.-K., Flammia, S. T., Becker, S., and Eisert, J. Quantum state tomography via compressed sensing. *Physical review letters*, 105(15):150401, 2010.

Guță, M. and Yamamoto, N. System identification for passive linear quantum systems. *IEEE Transactions on Automatic Control*, 61(4):921–936, 2016.

Hazan, E. *Introduction to Online Convex Optimization*. MIT Press, 2nd edition, 2022.

Hazan, E., Singh, K., and Zhang, C. Learning linear dynamical systems via spectral filtering. *Advances in Neural Information Processing Systems*, 30, 2017.

Hazan, E., Shwartz, S. S., and Srebro, N. Research program: Theory of learning in dynamical systems. *arXiv preprint arXiv:2512.19410*, 2025.

Huang, H.-Y., Kueng, R., and Preskill, J. Predicting many properties of a quantum system from very few measurements. *Nature Physics*, 16(10):1050–1057, 2020.

Levitt, M. and Gută, M. Identification of single-input–single-output quantum linear systems. *Physical Review A*, 95(3):033825, 2017.

Li, K., Xue, S., et al. Quantum linear system algorithm for general matrices in system identification. *Entropy*, 24(7):893, 2022.

Marsden, A. and Hazan, E. Universal sequence preconditioning. *arXiv preprint arXiv:2502.06545*, 2025.

Nielsen, M. A. and Chuang, I. L. *Quantum computation and quantum information*. Cambridge university press, 2010.

Nurdin, H. I., James, M. R., and Doherty, A. C. Network synthesis of linear dynamical quantum stochastic systems. *SIAM Journal on Control and Optimization*, 48(4):2686–2718, 2009.

Orvieto, A., De, S., Gulcehre, C., Pascanu, R., and Smith, S. L. Universality of linear recurrences followed by non-linear projections: finite-width guarantees and benefits of complex eigenvalues. *arXiv preprint arXiv:2307.11888*, 2023.

Ran-Milo, Y., Lumbroso, E., Cohen-Karlik, E., Giryes, R., Globerson, A., and Cohen, N. Provable benefits of complex parameterizations for structured state space models. *Advances in Neural Information Processing Systems*, 37:115906–115939, 2024.

Slepian, D. Prolate spheroidal wave functions, fourier analysis, and uncertainty—V: The discrete case. *Bell System Technical Journal*, 57(5):1371–1430, 1978. doi: 10.1002/j.1538-7305.1978.tb02104.x.

Wiseman, H. M. and Milburn, G. J. *Quantum measurement and control*. Cambridge university press, 2009.

A. Lower bounds for learning an LDS

In this section we establish a simple lower bound for learning a linear dynamical system with hidden dimension d (which can be thought of as W in the earlier notation of this paper), if we don't restrict β . This shows that our refined bounds require a bound on β .

While we construct a specific hard instance to prove the $\Omega(d)$ bound, the paper of (François et al., 2025) provides a more refined lower bound, but one based on stricter assumptions. Specifically, they show a granular lower bound of $1 - S/K$ for the task of learning a time-shift of K with state dimension S on white noise, further illustrating the necessity of spectral constraints (small β) for efficient learning. Their lower bound, however, restricts the model class to linear recurrent filters, whereas our bound applies to any learning algorithm.

Theorem A.1. *For any online learning algorithm \mathcal{A} , there exists a linear dynamical system (A, B, C, D) with hidden state dimension d , and a sequence of observations, such that the expected cumulative squared loss of \mathcal{A} over $T \geq d$ rounds is at least $\Omega(d)$.*

Proof. We construct a specific autonomous LDS where predicting the observations is information-theoretically equivalent to predicting a sequence of independent fair coin flips.

Consider an autonomous LDS defined by state dimension d , input dimension 0 (so $B = 0, D = 0$), and output dimension 1. The dynamics are given by:

$$\begin{aligned} h_{t+1} &= Ah_t \\ y_t &= Ch_t \end{aligned}$$

Let A be the cyclic permutation matrix that shifts vector components one position to the left:

$$A = \begin{pmatrix} 0 & 1 & 0 & \cdots & 0 \\ 0 & 0 & 1 & \cdots & 0 \\ \vdots & \vdots & \vdots & \ddots & \vdots \\ 0 & 0 & 0 & \cdots & 1 \\ 1 & 0 & 0 & \cdots & 0 \end{pmatrix}$$

Let C be the projection onto the first coordinate:

$$C = (1 \ 0 \ \cdots \ 0)$$

The initial state $h_0 \in \{-1, 1\}^d$ is chosen uniformly at random. This means each component $(h_0)_i$ is an independent Rademacher random variable, with $\mathbb{P}((h_0)_i = 1) = \mathbb{P}((h_0)_i = -1) = 1/2$.

At any time step $t \geq 0$, the state is $h_t = A^t h_0$ and the observation is $y_t = CA^t h_0$. Due to the structure of A and C , for the first d rounds $t \in \{0, 1, \dots, d-1\}$, we have precisely:

$$y_t = (h_0)_{t+1}$$

That is, the observation at time t reveals exactly the $(t+1)$ -th component of the initial unknown state vector h_0 .

For any deterministic online learning algorithm \mathcal{A} , its prediction \hat{y}_t at time t is a function only of past observations:

$$\hat{y}_t = f_t(y_0, y_1, \dots, y_{t-1})$$

Substituting our relation $y_i = (h_0)_{i+1}$, this means \hat{y}_t depends only on the first t components of h_0 :

$$\hat{y}_t = f_t((h_0)_1, (h_0)_2, \dots, (h_0)_t)$$

However, the true label y_t is $(h_0)_{t+1}$, which is statistically independent of the variables $(h_0)_1, \dots, (h_0)_t$. Consequently, $\mathbb{E}[y_t | y_0, \dots, y_{t-1}] = \mathbb{E}[(h_0)_{t+1}] = 0$.

The expected squared loss at any round $t < d$ is bounded from below:

$$\begin{aligned}\mathbb{E}[(y_t - \hat{y}_t)^2] &= \mathbb{E}[y_t^2 - 2y_t\hat{y}_t + \hat{y}_t^2] \\ &= \mathbb{E}[y_t^2] - 2\mathbb{E}[y_t]\mathbb{E}[\hat{y}_t] + \mathbb{E}[\hat{y}_t^2] \quad (\text{by independence}) \\ &= 1 - 0 + \mathbb{E}[\hat{y}_t^2] \\ &\geq 1\end{aligned}$$

Summing this expected loss over the first d rounds yields a total expected loss for the algorithm of at least d . Since the system is deterministic given h_0 , the best expert in hindsight (knowing h_0) achieves a total loss of 0. Therefore, the expected regret is at least $d - 0 = d$. \square

B. Proof of Theorem 3.2: Spectral Decay via Hadamard Products

This appendix gives a proof of Theorem 3.2, establishing stretched-exponential spectral decay governed by the effective dimension k^* . The matrix is decomposable as a Hadamard product of a Hankel matrix and the so-called Slepian matrix. The theorem combines the work of (Beckermann & Townsend, 2017) and (Hazan et al., 2017) which show the decay of the Hankel matrix and the work of Slepian which characterizes the spectrum of the DPSS matrix. We provide a critical lemma on the spectrum of the Hadamard product of two PSD matrices to get the final result.

B.1. A General Hadamard Eigenvalue Tail Bound

Lemma B.1 (Generalized Hadamard Eigenvalue Decay). *Let $A, B \in \mathbb{C}^{n \times n}$ be Hermitian positive semi-definite matrices with eigenvalues $\lambda_1 \geq \lambda_2 \geq \dots \geq 0$. For any integers $k, h \geq 1$, the $(kh + 1)$ -th eigenvalue of their Hadamard product $A \circ B$ satisfies*

$$\lambda_{kh+1}(A \circ B) \leq \lambda_1(B) \text{Tr}(A_{>k}) + \lambda_1(A) \text{Tr}(B_{>h}) + \text{Tr}(A_{>k}) \text{Tr}(B_{>h}), \quad (11)$$

where $\text{Tr}(M_{>r}) := \sum_{j=r+1}^n \lambda_j(M)$ denotes the tail sum.

Proof. Let

$$A = \sum_j \mu_j u_j u_j^\dagger, \quad B = \sum_i \zeta_i w_i w_i^\dagger$$

be eigendecompositions. Decompose

$$A = A_{\leq k} + A_{>k}, \quad B = B_{\leq h} + B_{>h}.$$

Then

$$A \circ B = \underbrace{A_{\leq k} \circ B_{\leq h}}_{M_1} + \underbrace{A_{>k} \circ B_{\leq h}}_{M_2} + \underbrace{A_{\leq k} \circ B_{>h}}_{M_3} + \underbrace{A_{>k} \circ B_{>h}}_{M_4}.$$

Rank bound.

$$M_1 = \sum_{j=1}^k \sum_{i=1}^h \mu_j \zeta_i (u_j \circ w_i) (u_j \circ w_i)^\dagger,$$

hence $\text{rank}(M_1) \leq kh$ and $\lambda_{kh+1}(M_1) = 0$.

Spectral bounds. Recall that Weyl's inequality states that

$$\lambda_{i+j-1}(A + B) \leq \lambda_i(A) + \lambda_j(B).$$

Therefore we have

$$\lambda_{kh+1}(A \circ B) \leq \lambda_{kh+1}(M_1) + \lambda_1(M_2 + M_3 + M_4) \leq \lambda_1(M_2) + \lambda_1(M_3) + \lambda_1(M_4).$$

In general it holds that for any PSD matrix P , non-negative ρ_i , and orthonormal vectors v_i

$$\lambda_1 \left(\sum_{i=1}^n \rho_i v_i v_i^\dagger \circ P \right) \leq \sum_{i=1}^n \rho_i \lambda_1(P).$$

Indeed, by Weyl's inequality we have

$$\lambda_1 \left(\sum_{i=1}^n \rho_i v_i v_i^\dagger \circ P \right) \leq \sum_{i=1}^n \lambda_1 \left(\rho_i v_i v_i^\dagger \circ P \right) = \sum_{i=1}^n \rho_i \lambda_1 \left(v_i v_i^\dagger \circ P \right).$$

For any PSD matrix P and vector v such that $\|v\|_2 \leq 1$ it is true that $\lambda_1(vv^\dagger \circ P) \leq \lambda_1(P)$. Indeed, if $D_v = \text{diag}(v)$ we can write $vv^\dagger \circ P$ as $D_v P D_v^\dagger$. Then

$$\lambda_1(D_v P D_v^\dagger) = \max_{x: \|x\|_2 \leq 1} x^\dagger (D_v P D_v^\dagger) x = \max_{y: \|D_v^\dagger y\| \leq 1} y^\dagger P y \leq \max_{y: \|y\|_2 \leq 1} y^\dagger P y = \lambda_1(P),$$

where the last inequality holds since $\|D_v\|_2 \leq 1$ and therefore whenever $\|y\|_2 \leq 1$ implies $\|D_v y\|_2 \leq 1$. Therefore we have,

$$\begin{aligned} \lambda_1(M_2) &\leq \text{Tr}(A_{>k}) \lambda_1(B), \\ \lambda_1(M_3) &\leq \text{Tr}(B_{>h}) \lambda_1(A), \\ \lambda_1(M_4) &\leq \text{Tr}(A_{>k}) \text{Tr}(B_{>h}). \end{aligned}$$

Summing completes the proof. \square

B.2. The Hankel Matrix Component

We borrow Lemma E.1 from [Hazan et al. \(2017\)](#) which is a result that largely follows from [\(Beckermann & Townsend, 2017\)](#).

Lemma B.2 (Lemma E.1 [\(Hazan et al., 2017\)](#)). *Let λ_j be the j -th top eigenvalue of A_T . Then for all $T \geq 10$,*

$$\lambda_j \leq \min \left(\frac{3}{4}, K \cdot c^{-j/\log T} \right) \quad (12)$$

B.3. The Prolate (DPSS) Component

This subsection states the spectral properties of the discrete prolate spheroidal sequence (DPSS) kernel, also called the “Slepian” as established in [\(Slepian, 1978\)](#) and its relation to the Toeplitz component of the Quantum Information Matrix.

Lemma B.3 (Identification with Slepian’s Prolate Matrix from [\(Slepian, 1978\)](#)). *Let $B \in \mathbb{C}^{W \times W}$ be the Toeplitz matrix with entries*

$$B_{jk} = 2\beta \text{sinc}((j-k)\beta), \quad j, k \in \{0, 1, \dots, W-1\},$$

where $\text{sinc}(x) = \sin(x)/x$ with $\text{sinc}(0) = 1$. Define $\beta_{\text{slep}} := \beta/(2\pi)$ and let $p(W, \beta_{\text{slep}}) \in \mathbb{R}^{W \times W}$ be Slepian’s prolate matrix with entries

$$p(W, \beta_{\text{slep}})_{jk} := \frac{\sin(2\pi\beta_{\text{slep}}(j-k))}{\pi(j-k)}, \quad (j \neq k), \quad p(W, \beta_{\text{slep}})_{jj} := 2\beta_{\text{slep}}.$$

Then

$$B = 2\pi p(W, \beta_{\text{slep}}).$$

In particular, the eigenvalues of B are exactly 2π times the eigenvalues $\lambda_k(W, \beta_{\text{slep}})$ studied by Slepian, and the associated eigenvectors are the discrete prolate spheroidal sequences (DPSS). Moreover, the Shannon number satisfies

$$2W\beta_{\text{slep}} = \frac{\beta}{\pi}W = k^*.$$

Proof. Using $\text{sinc}(x) = \sin(x)/x$, for $j \neq k$ we have

$$B_{jk} = 2\beta \cdot \frac{\sin((j-k)\beta)}{(j-k)\beta} = 2 \cdot \frac{\sin((j-k)\beta)}{(j-k)} = 2\pi \cdot \frac{\sin(2\pi\beta_{\text{slep}}(j-k))}{\pi(j-k)} = 2\pi p(W, \beta_{\text{slep}})_{jk},$$

where we used $\beta = 2\pi\beta_{\text{slep}}$. On the diagonal, $B_{jj} = 2\beta$ and $2\pi p_{jj} = 2\pi(2\beta_{\text{slep}}) = 4\pi\beta_{\text{slep}} = 2\beta$. The Shannon number identity follows immediately. \square

Theorem B.4 (DPSS Spectral Concentration and Cutoff (Slepian, 1978)). *Let B be as in Lemma B.3, and let*

$$k^* := \frac{\beta}{\pi} W.$$

Then the spectrum of B exhibits a sharp concentration phenomenon: there exist constants $c, C > 0$ (depending only on the bandwidth fraction β_{slep}) such that

- (Passband) *For $k \leq (1 - c) k^*$,*

$$\lambda_k(B) \geq 2\pi(1 - e^{-cW}).$$

- (Stopband) *For $k \geq (1 + c) k^*$,*

$$\lambda_k(B) \leq 2\pi e^{-cW}.$$

In particular there is a universal constant $c' > 0$ such that

$$\sum_{k > k^*} \lambda_k(B) \leq e^{-c'W}.$$

B.4. Spectral Decay for Slepian–Hankel Products

We now combine the Hadamard tail bound (Lemma B.1) with the Hankel concentration (Lemma B.2) and the DPSS concentration (Theorem B.4) to obtain the spectral decay of the Quantum Information Matrix $Z_W(\beta) = A \circ B$. Theorem 3.2 follows directly from the Theorem below.

Theorem B.5 (Slepian–Hadamard Spectral Decay). *Let $A, B \in \mathbb{C}^{n \times n}$ be Hermitian PSD matrices satisfying:*

1. **Hankel decay:** *There exist universal constants $C, \alpha > 0$ such that $\lambda_j(A) \leq Ce^{-\alpha j}$ for all $j \geq 1$.*

2. **Slepian structure:** *B has effective rank k^* in the sense that for some universal constants $C', c' > 0$*

$$\lambda_j(B) \leq C' \quad (j \leq k^*), \quad \sum_{j > k^*} \lambda_j(B) \leq e^{-c'W}.$$

Then there are universal constants $K, \alpha > 0$ such that for all $s \geq 1$,

$$\lambda_{sk^*+1}(A \circ B) \leq K e^{-\alpha s}. \quad (13)$$

In particular, for any k such that $k^ \leq k \leq W$ we have*

$$\lambda_k(A \circ B) \leq K \exp(-\alpha \lfloor k/k^* \rfloor).$$

Proof. Apply Lemma B.1 with cutoffs

$$h = s, \quad k = k^*.$$

Then $kh + 1 = sk^* + 1$ and

$$\lambda_{sk^*+1}(A \circ B) \leq \lambda_{\max}(B) \text{Tr}(A_{>s}) + \lambda_{\max}(A) \text{Tr}(B_{>k^*}) + \text{Tr}(A_{>s}) \text{Tr}(B_{>k^*}).$$

By the Hankel decay assumption,

$$\text{Tr}(A_{>s}) \leq 2Ce^{-\alpha s},$$

and by Theorem B.4,

$$\text{Tr}(B_{>k^*}) \leq e^{-c'W}.$$

Substituting yields

$$\lambda_{sk^*+1}(A \circ B) \leq 2CC'e^{-\alpha s} + Ce^{-c'W} + 2Ce^{-\alpha s}e^{-c'W}.$$

Since $s \leq W$ we can modify α to ensure the above expression is bounded by

$$Ke^{-\alpha's}.$$

To get the final result we set $s = \lfloor k/k^* \rfloor$ and note that since the eigenvalues are assumed to be sorted in descending order then $\lambda_{k+1} \leq \lambda_{(\lfloor k/k^* \rfloor)k^*+1}$. \square

C. Derivation of the Linear Response Representation

In the main text, we treat the quantum system abstractly as a high-dimensional Linear Time-Invariant (LTI) system. In this appendix, we provide the physical derivation of this model, starting from the fundamental laws of quantum mechanics and applying Linear Response Theory.

C.1. The Physical Formulation

The state of a d -dimensional quantum system is described by a density matrix $\rho_t \in \mathbb{C}^{d \times d}$, which is a positive semi-definite matrix with unit trace. In the most general setting (open quantum systems), the time evolution is given by a Quantum Channel (a completely positive trace-preserving map) \mathcal{E}_t . If the system is driven by a scalar classical control signal u_t , the dynamics evolve as:

$$\rho_{t+1} = \mathcal{E}(\rho_t, u_t). \quad (14)$$

A standard realization of this control setting is a system governed by a Hamiltonian containing a drift term H_0 and a control term H_c :

$$H(u_t) = H_0 + u_t H_c. \quad (15)$$

For a closed system, the channel \mathcal{E} corresponds to unitary conjugation. Over a time step δt (assuming $\hbar = 1$), the update is:

$$\rho_{t+1} = e^{-i(H_0+u_t H_c)\delta t} \rho_t e^{i(H_0+u_t H_c)\delta t}. \quad (16)$$

We do not observe the state ρ_t directly. Instead, we measure an observable operator O , yielding the expectation value:

$$y_t = \text{Tr}(O \rho_t). \quad (17)$$

Equation (16) represents the "Physical Formulation." It is bilinear in the state ρ and the unitary operator (which depends on u), making it difficult to learn directly.

C.2. Linear Response Theory

To bridge the gap between the physical dynamics and the LTI formulation, we employ Linear Response Theory. We assume the system operates near a steady state equilibrium ρ_{ss} (where $\rho_{ss} = \mathcal{E}(\rho_{ss}, 0)$) and that the control signals u_t are small perturbations.

We perform a first-order Taylor expansion of the channel $\mathcal{E}(\rho, u)$ around the point $(\rho, u) = (\rho_t, 0)$:

$$\rho_{t+1} \approx \mathcal{E}(\rho_t, 0) + u_t \cdot \frac{\partial \mathcal{E}}{\partial u}(\rho_{ss}, 0). \quad (18)$$

Here, the first term represents the *free evolution* of the current state, and the second term represents the *driven evolution*, where we approximate the state acting on the control derivative as the steady state ρ_{ss} .

C.3. Vectorization to LTI

To convert this linearized matrix equation into the standard vector form used in Eq. (1), we use the *Liouville Space* formalism. We define the vectorization map $|\cdot\rangle\rangle : \mathbb{C}^{d \times d} \rightarrow \mathbb{C}^{d^2}$ which stacks the columns of a matrix into a single column vector. Using the algebraic identity $|XYZ\rangle\rangle = (Z^\top \otimes X)|Y\rangle\rangle$, we can identify the LTI system matrices (A, B, C) :

1. The State Transition Matrix (A). The free evolution term $\mathcal{E}(\rho_t, 0)$ is linear in ρ_t . For the unitary case $\rho \mapsto e^{-iH_0\delta t} \rho e^{iH_0\delta t}$, the vectorized action is:

$$A \triangleq e^{iH_0^\top \delta t} \otimes e^{-iH_0\delta t}. \quad (19)$$

This superoperator $A \in \mathbb{C}^{d^2 \times d^2}$ is the Liouvillian of the system. Its eigenvalues determine the spectral properties of the dynamics (i.e., the sector \mathbb{C}_β).

From Eq. (19), the eigenvalues of the Liouvillian superoperator A are given by $\lambda_{jk} = e^{i(E_j - E_k)\delta t}$, where E_j, E_k are the eigenvalues of the Hamiltonian H_0 . The spectral bound $|\arg(z)| \leq \beta$ therefore imposes a constraint on the system's maximum Bohr frequency relative to the sampling rate:

$$\max_{j,k} |E_j - E_k| \delta t \leq \beta \quad (20)$$

This inequality provides the physical interpretation of β : it is the product of the maximum energy gap (bandwidth) of the system and the sampling interval δt . To satisfy the stability condition, the sampling rate must be sufficiently high to resolve the fastest dynamics within the sector β .

2. The Control Matrix (B). The control term depends on the derivative of the unitary with respect to u . In the limit of small δt , this corresponds to the commutator with the control Hamiltonian. The vector B captures the excitation of the steady state by the control:

$$B \triangleq \left| \frac{\partial \mathcal{E}}{\partial u}(\rho_{ss}) \right\rangle \in \mathbb{C}^{d^2}. \quad (21)$$

Physically, B represents how the control field "injects" information into the state space.

3. The Observation Matrix (C). Using the Hilbert-Schmidt inner product $\text{Tr}(X^\dagger Y) = \langle\langle X | Y \rangle\rangle$, the observation equation becomes:

$$y_t = \text{Tr}(O\rho_t) = \langle\langle O^\dagger | \rho_t \rangle\rangle \implies C \triangleq |O^\dagger\rangle\rangle^\dagger. \quad (22)$$

C.4. Summary of Transformation

Combining these steps, we recover the high-dimensional LTI system described in the Introduction:

$$\begin{aligned} h_{t+1} &= Ah_t + Bu_t \\ y_t &= Ch_t, \end{aligned}$$

where $h_t = |\rho_t\rangle\rangle$. This derivation highlights the **Curse of Dimensionality**: if the physical system has Hilbert dimension d (e.g., $d = 2^n$ for n qubits), the LTI state h_t has dimension $d^2 = 4^n$. Our algorithm's independence from the hidden dimension corresponds physically to learning the dynamics without reconstructing the full $4^n \times 4^n$ Liouvillian superoperator.